Erzincan Üniversitesi
Fen Bilimleri Enstitüsü Dergisi
2020, 13(1), 181-189
ISSN: 1307-9085, e-ISSN: 2149-4584
Araştırma Makalesi

Erzincan University
Journal of Science and Technology
2020, 13(1), 181-189
DOI: 10.18185/erzifbed.623764
Research Article

The Effect of Cu doping on Fatigue Properties of TiZrNbN Coatings

Hossein AHMAD AGHDAM[1], Aysenur KELES[1*], Ozlem BARAN[2],

Yasar TOTIK[1], Ihsan EFEOGLU[1]

[1]Atatürk University, Faculty of Engineering, Erzurum, Turkey
[1]Erzincan University, Faculty of Engineering, Erzincan, Turkey

Geliş / Received: 24/09/2019, Kabul / Accepted: 29/01/2020

Abstract

The fatigue properties are very important for cutting tools due to service life. To improve fatigue properties of cutting tools, transition metal nitrides with soft metal (Cu, Ni etc.) have been coated on cutting tool materials. To investigate Cu effect on fatigue properties, TiZrNbN and Cu doped TiZrNbN coatings were deposited on M2 high speed steel using reactive closed field unbalanced magnetron sputtering (CFUBMS) in bias voltage of -80V, coating pressure of 0.33 Pa and Cu target current of 0.6 A. Microstructure properties of the coatings were determined by X-Ray Diffraction (XRD), Scanning Electron Microscope (SEM) and Energy Dispersive Spectroscopy (EDS). Mechanical properties of the coatings were examined with microhardness tester and scratch tester. Fatigue properties of the coatings were examined using multi-pass scratch tester. According to the results, the microhardness of Cu doped TiZrNbN is better than TiZrNbN. On the other hand, the adhesion and fatigue properties of TiZrNbN are the highest.

Keywords: CFUBMS, multi-pass scratch, TiZrNbN, fatigue, Cu

Cu ilavesinin TiZrNbN Kaplamaların Yorulma Özelliklerine Etkisi

Öz

Yorulma özellikleri, kullanım ömrü nedeniyle kesme aletleri için çok önemlidir. Kesici takımların yorulma özelliklerini iyileştirmek için kesici takım malzemeleri üzerine yumuşak metalle (Cu, Ni vb.) Geçiş metali nitrürleri kaplanmıştır. Yorulma özellikleri üzerindeki Cu etkisini araştırmak için, TiZrNbN ve Cu katkılı TiZrNbN kaplamalar, -80V'luk ön gerilim voltajında, 0.33 Pa'lık kaplama basıncı ve Cu hedef akımında 0.6 A değerinde reaktif kapalı alan dengesiz manyetik alanda sıçratma (CFUBMS) kullanılarak M2 yüksek hızlı çelik üzerinde biriktirildi. Kaplamaların mikro yapı özellikleri X-Ray Difraktometri (XRD), Taramalı Elektron Mikroskop (SEM) ve Enerji Dağıtıcı Spektroskopi (EDS) ile belirlenmiştir. Kaplamaların mekanik özellikleri microhardness test cihazı ve çizik test cihazı ile incelenmiştir. Kaplamaların yorulma özellikleri çok geçişli çizik test cihazı kullanılarak incelenmiştir. Sonuçlara göre, Cu katkılı TiZrNbN'nin mikro sertliği TiZrNbN'den daha iyidir. Öte yandan, TiZrNbN'nin yapışma ve yorulma özellikleri en yüksektir.

Anahtar Kelimeler: CFUBMS, çoklu geçişli çizik, TiZrNbN, yorulma, Cu

*Corresponding Author: aysenur.keles@atauni.edu.tr

1. Introduction

Transition metal nitride films use to improve wear resistance, fatigue strength and mechanical properties of materials (Baran, Keles, Cicek, Totik, & Efeoglu, 2017; Bidev, Baran, Arslan, Totik, & Efeoglu, 2013; Bloyce, Qi, Dong, & Bell, 1998; Stallard, Poulat, & Teer, 2006). These films are becoming more important for industrial application in cutting tools and hot working application because of their good mechanical properties (high hardness and adhesion) and excellent tribological properties (low friction coefficient (CoF), high wear resistance) (Grimberg, Zhitomirsky, Boxman, Goldsmith, & Weiss, 1998; Keles, Cicek, Baran, Totik, & Efeoglu, 2017; Latella, Gan, Daviesb, McKenzie, & McCulloch, 2006; Montero-Ocampo, Ramirez-Ceja, & Hidalgo-Badillo, 2015).

A lot of vacuum deposition methods such as pulsed laser deposition (PLD) (Fominski, Grigoriev, Celis, Romanov, & Oshurko, 2012), thermal reactive deposition (Alajlani et al., 2016), plasma-assisted chemical vapor deposition (PA-CVD) (Movassagh-Alanagh, Abdollah-Zadeh, Aliofkhazraei, & Abedi, 2017), magnetron sputtering (Ye & Sun, 2018) are used to deposit multifunctional nanocomposite films. Closed field unbalanced magnetron sputtering (CFUBMS) is a common process and successful technology to deposit of transition metal nitride coatings. With help of this deposition method, improved adhesion between coating and substrate, uniformly and obtain a lower residual stress, because of improving the effectiveness of precleaning and the performance of deposition coating by applying pulsed-dc bias to substrate (Gangopadhyay, Acharya, Chattopadhyay, & Paul, 2010; Kara, Kucukomeroglu, Baran, Efeoglu, & Yamamoto, 2014; Kelly & Arnell, 2000).

TiN is one of most popular film and commonly used on metal tools, nevertheless, properties of these films have still some weakness including adhesion, friction, and corrosion resistance. The researchers focus on added mainly transition metals such as Zr, Nb, Al and Cu to form ternary, quaternary, composite and nanocomposite structure to enhance fatigue behavior, attain low friction and good adhesion (Grimberg, et al., 1998; Kara, et al., 2014; Montero-Ocampo, et al., 2015; Pogrebnjak et al., 2017).

For measurement of the adhesion between protective coatings and substrate using various test methods such as pull-off test, laser technique, acoustic imaging, indentation and scratch test (Du, Tittmann, & Ju, 2010; Fizi, Mebdoua, Lahmar, Djeraf, & Benbahouche, 2015; Qiu & Lau, 2017; Sadowski, Hola, Czarnecki, & Wang, 2018; Stallard, et al., 2006). As far as known, adhesion of coatings is commonly evaluated using scratch test. For the first time, a scratch test was performed by Heaven in 1950 (Heavens, 1950). During scratch test, normal load is linearly raised from minimum to maximum values. The load value cause to the coating rupture from the substrate is defined as critical load. Multi-pass scratch test was carried out firstly by Bull and Rickerby to obtain information about the wear and fatigue behavior of the coatings. In this test, a constant load with multi-scratch is applied to the coatings for determining fatigue behavior (Bull & Rickerby, 1989).

Fatigue failure is a common phenomenon for protective coatings and playing an important role on coating life (Rodriguez-Castro et al., 2016; von Stebut, 2005; Yildiz & Alsaran, 2010). Fatigue properties of coatings were

generally evaluated by using multi-pass scratch test. Efeoglu et al. (Efeoglu & Arnell, 2000) studied fatigue properties of TiN coatings using multi-pass scratch test at sub-critical loads and reported that the coatings did have no adhesive and cohesive failures at sub-critical loads. Stallard et al. (Stallard, et al., 2006) investigated the adhesion properties of TiN coating on ASP23 HSS and TA46 titanium alloy. They showed that TiN coating on titanium alloy had lower fatigue and adhesive failures than TiN coating on steel. In the literature, only one study has been done about the ZrTiNbN coatings (Pogrebnjak, et al., 2017) but there is no research reported about the fatigue properties of TiZrNbN and Cu doped TiZrNbN coatings. The main aim of this study was investigated adhesion and fatigue behavior of TiZrNbN and Cu doped TiZrNbN using scratch test and multi-pass scratch test, respectively.

2. Material and Methods

In this study, AISI M2 (C 0.8 wt.%, Si 0.30 wt.%, Cr 4.2 wt.%, Mn 0.30 wt.%, Mo 5.1 wt.%, W 6.3 wt.%, and V 1.95-2 wt.% and Fe balance) high speed steel was chosen a substrate. To deposit TiZrNbN and Cu doped TiZrNbN coatings were used reactive pulsed-dc CFUBMS (Teer coating Ltd. UPD 500). Before process, the substrate surfaces were rubbed with SiC emery paper to reach roughness value of Ra≈0.1μm and cleaned with ethanol in an ultrasonic bath for 10 minutes and then dried with a hot air fan.

To deposit TiZrNbN and Cu doped TiZrNbN coatings, one Ti target (%99.99), one Zr target (%99.99), one Nb target (%99.99), and one Cu target (%99.99) were used in the coating chamber. Target dimension is 345* 145* 6 mm. The distance between the substrate and each target is 70 mm. Ar and N2 gases were used for ionization and reactive coating, respectively. Base pressure before deposition is 0.0026 Pa. At the beginning of the deposition process, to remove contaminations on the substrate surface and improve adhesion between the coating and substrate, ion cleaning was in progress by a pressure 0.30 Pa with argon gas in 20 minutes. Ti interlayer (~50nm) was deposited in 5 minutes to minimize residual stress and increase adhesion between the coating and substrate. After Ti interlayer, the TiZrNbN and Cu doped TiZrNbN coatings were coated by substrate bias voltage of -80 V, the Zr and Nb target currents of 5 A, the Ti current of 3 A, the N2 flow rate of 12 sccm, the working pressure of 0.33 Pa and deposition time of 45 minutes. Additionally, for Cu doped TiZrNbN coating, the Cu target current was set to 0.6 A.

The crystal structure of the coatings was examined by X-ray Diffractometer (XRD) (Rigaku-2200 D/Max) with Cu-Kα (λ= 0.154 nm) radiation source over the 2θ range of 30–70° (with a step size of 0.1°). The grain size of the coatings was calculated using Scherrer formula.

The morphology and elemental analyses of the coatings were determined using scanning electron microscope (SEM) (FEI Quanta FEG-450) and energy dispersive spectroscopy (EDS), respectively.

The microhardness value of the TiZrNbN and Cu doped TiZrNbN coatings was obtained by Knoop microhardness measurements using a Buehler microhardness tester under a load of 10 gf for 15 s. Penetration depth is %10 lower than films thickness.

To determine the adhesion properties of the TiZrNbN and Cu doped TiZrNbN coatings, a scratch tester produced by Anton Paar Revetester Instruments (formerly CSM) was

used. The critical load values were measured by a Rockwell-C diamond indenter with a 200 µm radius hemispherical tip under a sliding speed of 10 mm/min. To assess the fatigue resistance of the coatings, bidirectional multi-pass scratch tests were performed on the same track. The multi-pass scratch tests were performed under three different sub-critical load values (15 N, 20 N and 25 N) with a Rockwell-C diamond indenter on 3 mm scratch tracks under 150 cycles.

3. Research Findings

SEM images for the cross-sectional and surface morphological of the TiZrNbN and Cu doped TiZrNbN coatings are shown in Fig.1. According to cross-sectional SEM images, the TiZrNbN and Cu doped TiZrNbN coatings thickness values are measured as 1.468 µm and 1.894 µm, respectively. The coating thickness values increase by addition of Cu due to the higher sputter yield.(Ezirmik & Rouhi, 2014). The TiZrNbN and Cu doped TiZrNbN coatings are exhibited dense-columnar and dense microstructures, respectively. According to chemical composition obtained from EDS analyses, content of elements for TiZrNbN coating (Fig.2) are 31.23 at. % N, 19.08 at. % Zr, 34.23 at. % Nb and 15.46 at. % Ti, for Cu doped TiZrNbN coating (Fig.3) are 43.33 at. % N, 16.88 at. % Zr, 27.25 at. % Nb, 11.98 at. % Ti and 0.52 at. % Cu.

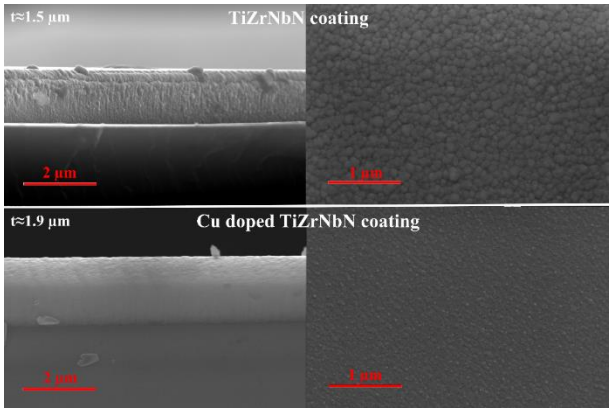

Figure 1. The cross-sectional and surface morphological SEM images of TiZrNbN and Cu doped TiZrNbN coatings

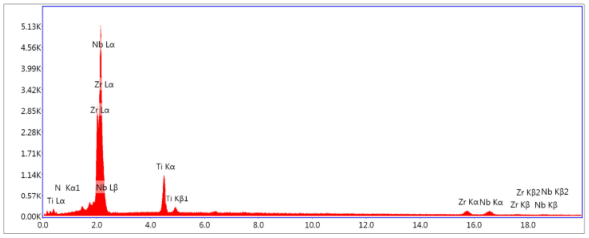

Figure2. EDS analysis for TiNbZrN coating

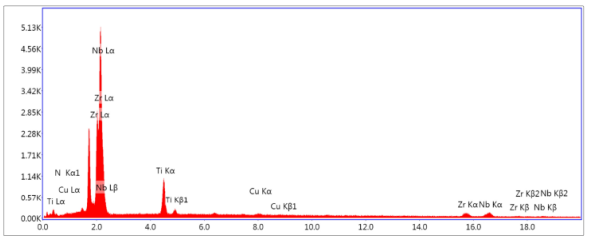

Figure 3. EDS analysis for Cu doped TiNbZrN

Fig.4 shows XRD pattern for the TiZrNbN and Cu doped TiZrNbN coatings. Both coatings have TiZrNbN (111), TiZrNbN (110) and TiZrNbN (300) phases (Pogrebnjak, et al., 2017). The dominant phases for both coatings are (111)-fcc and (110)-bcc phases. The grain size was calculated as 25 nm and 12.3 nm for the TiZrNbN and Cu doped TiZrNbN coatings, respectively. With Cu doped, the intensity of phases has increased and the grain sizes have decreased. The increasing (111) phase intensity in Cu doped TiZrNbN coating

is efficacious on decreasing grain size (Musil, 2000). Also, the decreasing grain size has caused the increasing hardness in Cu doped TiZrNbN coating (51 GPa). Veprek and Reiprich (Veprek & Reiprich, 1995) reported that is a similar effect. The hardness value has been obtained as 21 GPa in TiZrNbN coating.

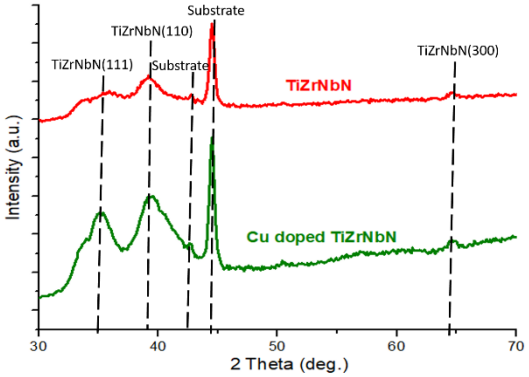

Figure 4. XRD patterns of TiZrNbN and Cu doped TiZrNbN coatings

The critical load values obtained from scratch tests for the TiZrNbN and Cu doped TiZrNbN coatings are 57N and 28N, respectively (Fig.5 (a) and (b)). The hardness values of TiZrNbN have increased with Cu doped, but the increment in hardness has resulted in the decrescent critical load. Also, the optical microscope images of scratch lines are shown in Fig.5 (a) and (b). As seen in Fig 5 (a), up to 15 N, there are no failures, but after this load value, adhesive failures occurred on TiZrNbN coating. In Fig. 5 (b), chevron cracks (Jacobs et al., 2003), adhesive failures (Keles, et al., 2017) and adhesive chippings (Gogotsi, 2013; Stallard, et al., 2006) in the scratch lines border took place on Cu doped TiZrNbN coating at 10 N. After 25 N, only adhesive failures as chipping shape were identified for Cu doped TiZrNbN coating.

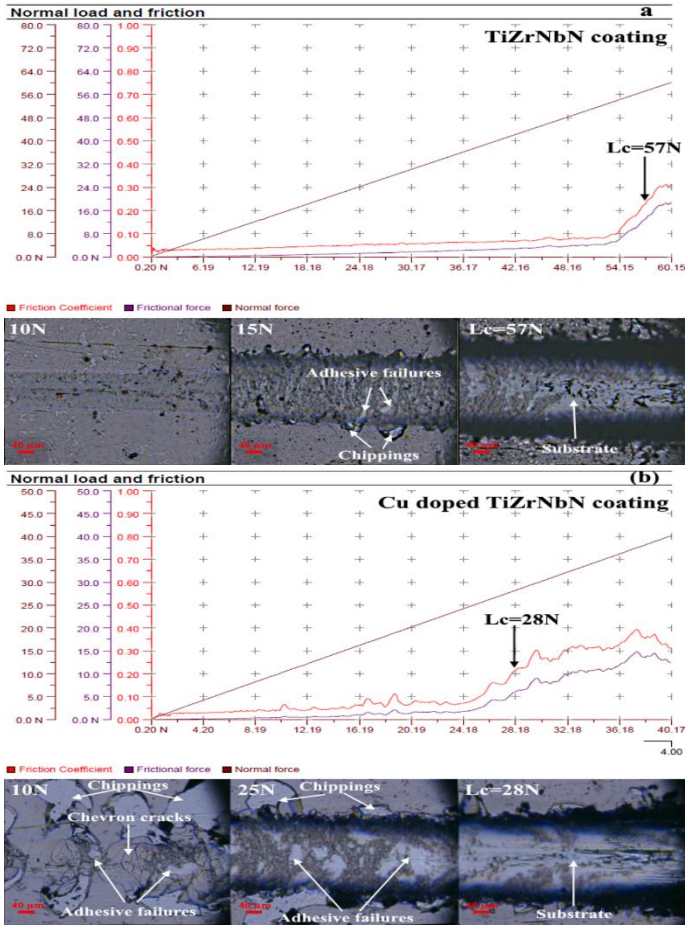

Figure 5. The critical load values obtained from scratch tests for the (a) TiZrNbN and (b) Cu doped TiZrNbN coatings

The fatigue performance of the TiZrNbN and Cu doped TiZrNbN coatings were characterized with multi-pass scratch test. Fig.6 shows the CoF-cycle graph for TiZrNbN and Cu doped TiZrNbN coatings under different loads. The mean CoF values under 15 N, 20 N and 25 N loads for TiZrNbN coating are 0.0162, 0.0192 and 0.03, respectively. On the other hand, for Cu doped TiZrNbN coating, the mean CoF values under 15 N, 20 N and 25 N loads are 0.02, 0.022 and 0.038, respectively. For TiZrNbN-Cu (at 15N, 20N) and TiZrNbN (at 15), the behavior of CoF is seen as fluctuation but they reached to steady state at higher cycles. For TiZrNbN (at 20N, 25N) and TiZrNbN-Cu (at 25N), in the first cycle have the higher coefficient and

then, gradually decrease subsequent cycles until the steady state is reached. When the indenter moves on the surface of the coating, scratches are formed in the first cycle without being dragged on the surface. However, other plastic deformation does not occur in the substrate and the CoF decreases (FischerCripps & Lawn, 1996; Kataria, Kumar, Dash, Ramaseshan, & Tyagi, 2010). Also, Fig 7 (a), (b) and (c) are connected with the optical microscope images of the scratch lines obtained from multi-pass scratch tests for TiZrNbN and TiZrNbN-Cu coatings under 15N, 20N and 25N loads, respectively. Compared to TiZrNbN coating, under 15N and 20N loads were observed more adhesive failures and chippings in the border of scratch line for Cu doped TiZrNbN coating. Under 25N load, the enormous adhesive failures occurred in Cu doped TiZrNbN coating. On the other hand, only adhesive failure in a few areas occurred in TiZrNbN coating.

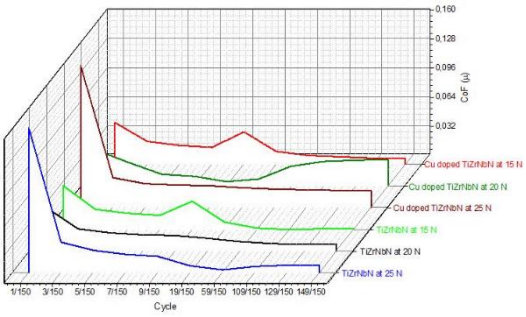

Figure 6. The cycle- CoF graph for TiZrNbN and TiZrNbN-Cu coatings under different loads

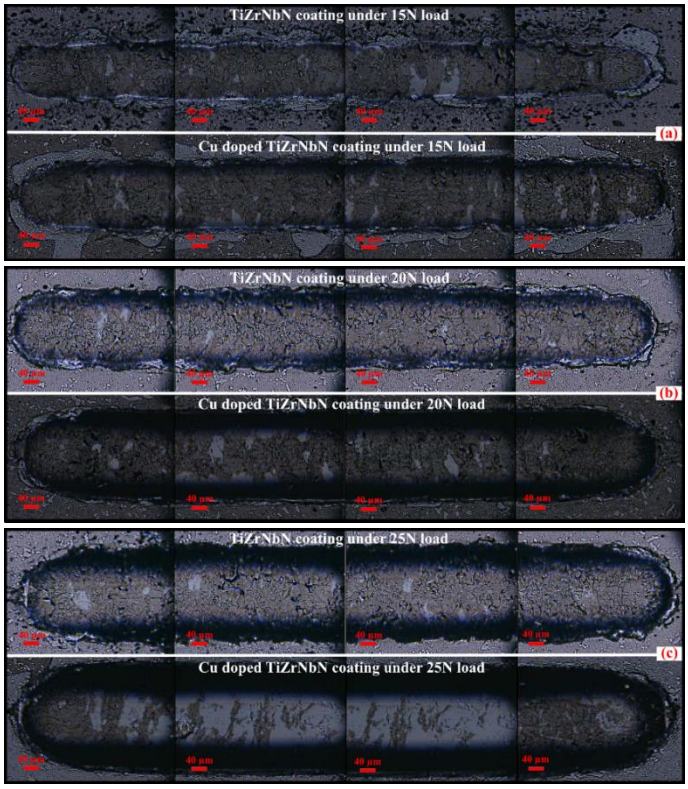

Figure 7. Optical microscope images of scratch scars obtained from multi-pass scratch tests for TiZrNbN and Cu doped TiZrNbN coatings under (a) 15N, (b) 20N and (c) 25N loads.

4. Results

The main results of this paper can be summed up as follows.

- The thickness values of TiZrNbN and Cu doped TiZrNbN coatings were 1.468 µm and 1.894 µm, respectively. The reason for the increase in thickness is the addition of Cu.
- TiZrNbN and Cu doped TiZrNbN coatings exhibited TiZrNbN (111), TiZrNbN (110) and TiZrNbN (300) phases. The intensity of TiZrNbN (111) in Cu doped TiZrNbN coating was higher than TiZrNbN coating. So, the grain size is twice smaller for Cu doped TiZrNbN coating when compared to TiZrNbN coating.

- The hardness is related to grain size. Therefore, the hardness of Cu doped TiZrNbN coating was higher than TiZrNbN coating. When Cu was doped to the TiNbZrN film, the hardness increased by about two times.

- Due to low hardness (21 GPa), TiZrNbN coating had higher critical load value than Cu doped TiZrNbN coating. All coatings exhibited adhesive failure. Also, the critical load was reduced approximately twice by the addition of Cu.

- A comparison was taken between TiZrNbN and Cu doped TiZrNbN coatings, the fatigue behavior was deteriorated with incorporating Cu. The CoF values were obtained higher at Cu doped TiZrNbN coating. Therefore, enormous adhesive failures occurred at Cu doped TiZrNbN coating.

5. References

Alajlani, Y., Placido, F., Gibson, D., Chu, H. O., Song, S. G., Porteous, L., & Moh, S. (2016). Nanostructured ZnO films prepared by hydro-thermal chemical deposition and microwave-activated reactive sputtering. *Surface & Coatings Technology, 290*, 16-20. doi: 10.1016/j.surfcoat.2016.01.036

Baran, O., Keles, A., Cicek, H., Totik, Y., & Efeoglu, I. (2017). The mechanical and tribological properties of Ti Nb, V N films on the Al-2024 alloy. [Article; Proceedings Paper]. *Surface & Coatings Technology, 332*, 312-318. doi: 10.1016/j.surfcoat.2017.06.088

Bidev, F., Baran, O., Arslan, E., Totik, Y., & Efeoglu, I. (2013). Adhesion and fatigue properties of Ti/TiB2/MoS2 graded-composite coatings deposited by closed-field unbalanced magnetron sputtering. *Surface & Coatings Technology, 215*, 266-271. doi: 10.1016/j.surfcoat.2012.08.091

Bloyce, A., Qi, P. Y., Dong, H., & Bell, T. (1998). Surface modification of titanium alloys for combined improvements in corrosion and wear resistance. *Surface & Coatings Technology, 107*(2-3), 125-132. doi: 10.1016/s0257-8972(98)00580-5

Bull, S. J., & Rickerby, D. S. (1989). MULTI-PASS SCRATCH TESTING AS A MODEL FOR ABRASIVE WEAR. *Thin Solid Films, 181*, 545-553. doi: 10.1016/0040-6090(89)90523-3

Du, J. K., Tittmann, B. R., & Ju, H. S. (2010). Evaluation of film adhesion to substrates by means of surface acoustic wave dispersion. *Thin Solid Films, 518*(20), 5786-5795. doi: 10.1016/j.tsf.2010.05.086

Efeoglu, I., & Arnell, R. D. (2000). Multi-pass sub-critical load testing of titanium nitride coatings. *Thin Solid Films, 377*, 346-353. doi: 10.1016/s0040-6090(00)01309-2

Ezirmik, K. V., & Rouhi, S. (2014). Influence of Cu additions on the mechanical and wear properties of NbN coatings. *Surface & Coatings Technology, 260*, 179-185. doi: 10.1016/j.surfcoat.2014.09.056

FischerCripps, A. C., & Lawn, B. R. (1996). Stress analysis of contact deformation in quasi-plastic ceramics. *Journal of the American Ceramic Society, 79*(10), 2609-2618.

Fizi, Y., Mebdoua, Y., Lahmar, H., Djeraf, S., & Benbahouche, S. (2015). Adhesion of FeCrNiBSi-(W-Ti)C wire-arc deposited coatings onto carbon steel substrates determined by indentation measurements and modeling. *Surface & Coatings Technology, 268*, 310-316. doi: 10.1016/j.surfcoat.2014.11.004

Fominski, V. Y., Grigoriev, S. N., Celis, J. P., Romanov, R. I., & Oshurko, V. B. (2012). Structure and mechanical properties of W-Se-C/diamond-like carbon and W-Se/diamond-like carbon bi-layer coatings prepared by pulsed laser deposition. *Thin Solid Films, 520*(21), 6476-6483. doi: 10.1016/j.tsf.2012.06.085

Gangopadhyay, S., Acharya, R., Chattopadhyay, A. K., & Paul, S. (2010). Effect of substrate bias voltage on structural and mechanical properties of pulsed DC magnetron sputtered TiN-MoSx composite coatings. *Vacuum, 84*(6), 843-850. doi: 10.1016/j.vacuum.2009.11.010

Gogotsi, G. A. (2013). Criteria of ceramics fracture (edge chipping and fracture toughness tests). *Ceramics International, 39*(3), 3293-3300. doi: 10.1016/j.ceramint.2012.10.017

Grimberg, I., Zhitomirsky, V. N., Boxman, R. L., Goldsmith, S., & Weiss, B. Z. (1998). Multicomponent Ti-Zr-N and Ti-Nb-N coatings deposited by vacuum arc. *Surface & Coatings Technology, 108*(1-3), 154-159. doi: 10.1016/s0257-8972(98)00658-6

Heavens, O. S. (1950). Some factors influencing the adhesion of films produced by vacuum evaporation. *Journal de Physique et le Radium, , 11*, 355-360.

Jacobs, R., Meneve, J., Dyson, G., Teer, D. G., Jennett, N. M., Harris, P., . . . Ingelbrecht, C. D. (2003). A certified reference material for the scratch test. *Surface & Coatings Technology, 174*, 1008-1013. doi: 10.1016/s0257-8972(03)00470-5

Kara, L., Kucukomeroglu, T., Baran, O., Efeoglu, I., & Yamamoto, K. (2014). Microstructure, Mechanical, and Scratch Resistance Properties of TiAlCrNbN-Graded Composite Coating Deposited on AISI H13 Steel Substrate with Pulsed DC Closed Field Unbalanced Magnetron Sputtering Method. *Metallurgical and Materials Transactions a-Physical Metallurgy and Materials Science, 45A*(4), 2123-2131. doi: 10.1007/s11661-013-2148-2

Kataria, S., Kumar, N., Dash, S., Ramaseshan, R., & Tyagi, A. K. (2010). Evolution of deformation and friction during multimode scratch test on TiN coated D9 steel. *Surface & Coatings Technology, 205*(3), 922-927. doi: 10.1016/j.surfcoat.2010.08.060

Keles, A., Cicek, H., Baran, O., Totik, Y., & Efeoglu, I. (2017). Determining the critical loads of V and Nb doped ternary TiN-based coatings deposited using CFUBMS on steels. *Surface & Coatings Technology, 332*, 168-173. doi: 10.1016/j.surfcoat.2017.07.085

Kelly, P. J., & Arnell, R. D. (2000). Magnetron sputtering: a review of recent developments and applications. *Vacuum, 56*(3), 159-172. doi: 10.1016/s0042-207x(99)00189-x

Latella, B. A., Gan, B. K., Daviesb, K. E., McKenzie, D. R., & McCulloch, D. G. (2006). Titanium nitride/vanadium nitride alloy coatings: mechanical properties and adhesion characteristics. *Surface & Coatings Technology, 200*(11), 3605-3611. doi: 10.1016/j.surfcoat.2004.09.008

Montero-Ocampo, C., Ramirez-Ceja, E. A., & Hidalgo-Badillo, J. A. (2015). Effect of codeposition parameters on the hardness and adhesion of TiVN coatings. *Ceramics International, 41*(9), 11013-11023. doi: 10.1016/j.ceramint.2015.05.046

Movassagh-Alanagh, F., Abdollah-Zadeh, A., Aliofkhazraei, M., & Abedi, M. (2017). Improving the wear and corrosion resistance of Ti-6Al-4V alloy by deposition of TiSiN nanocomposite coating with pulsed-DC PACVD. *Wear, 390-391*, 93-103. doi: 10.1016/j.wear.2017.07.009

Musil, J. (2000). Hard and superhard nanocomposite coatings. *Surface & Coatings Technology, 125*(1-3), 322-330. doi: 10.1016/s0257-8972(99)00586-1

Pogrebnjak, A. D., Bagdasaryan, A. A., Beresnev, V. M., Nyemchenko, U. S., Ivashchenko, V. I., Kravchenko, Y. O., . . . Maksakova, O. (2017). The effects of Cr and Si additions and deposition conditions on the structure and properties of the (Zr-Ti-Nb)N coatings. *Ceramics International, 43*(1), 771-782. doi: 10.1016/j.ceramint.2016.10.008

Qiu, Q. W., & Lau, D. V. (2017). A novel approach for near-surface defect detection in FRP-bonded concrete systems using laser reflection and acoustic-laser techniques. *Construction and Building Materials, 141*, 553-564. doi: 10.1016/j.conbuildmat.2017.03.024

Rodriguez-Castro, G. A., Vega-Moron, R. C., Meneses-Amador, A., Jimenez-Diaz, H. W., Andraca-Adame, J. A., Campos-Silva, I. E., & Pardave, M. E. P. (2016). Multi-pass scratch test behavior of AISI 316L borided steel. *Surface & Coatings Technology, 307*, 491-499. doi: 10.1016/j.surfcoat.2016.09.017

Sadowski, L., Hola, J., Czarnecki, S., & Wang, D. H. (2018). Pull-off adhesion prediction of variable thick overlay to the substrate. *Automation in Construction, 85*, 10-23. doi: 10.1016/j.autcon.2017.10.001

Stallard, J., Poulat, S., & Teer, D. G. (2006). The study of the adhesion of a TiN coating on steel and titanium alloy substrates using a multi-mode scratch tester. *Tribology International, 39*(2), 159-166. doi: 10.1016/j.triboint.2005.04.011

Veprek, S., & Reiprich, S. (1995). A concept for the design of novel superhard coatings. *Thin Solid Films, 268*(1-2), 64-71. doi: 10.1016/0040-6090(95)06695-0

von Stebut, J. (2005). Multi-mode scratch testing - a European standards, measurements and testing study. *Surface & Coatings Technology, 200*(1-4), 346-350. doi: 10.1016/j.surfcoat.2005.02.055

Ye, F. X., & Sun, X. (2018). Nanoindentation response analysis of TiN-Cu coating deposited by magnetron sputtering. *Progress in Natural Science-Materials International, 28*(1), 40-44. doi: 10.1016/j.pnsc.2018.01.001

Yildiz, F., & Alsaran, A. (2010). Multi-pass scratch test behavior of modified layer formed during plasma nitriding. *Tribology International, 43*(8), 1472-1478. doi: 10.1016/j.triboint.2010.02.005

.